

Title	Enhanced skin deposition and delivery of voriconazole using ethosomal preparations.
Authors	Faisal, Waleed;Soliman, Ghareb M;Hamdan, Ahmed M
Publication date	2016-09-25
Original Citation	Faisal, W., Soliman, G. M. and Hamdan, A. M. (2018) 'Enhanced skin deposition and delivery of voriconazole using ethosomal preparations', Journal of Liposome Research, 28(1), pp. 14-21. doi: 10.1080/08982104.2016.1239636
Type of publication	Article (peer-reviewed)
Link to publisher's version	<a href="https://www.tandfonline.com/doi/full/10.1080/08982104.2016.1239636">https://www.tandfonline.com/doi/full/10.1080/08982104.2016.1239636</a> - 10.1080/08982104.2016.1239636
Rights	© 2016 Informa UK Ltd. Trading as Taylor & Francis. This is an Accepted Manuscript of an article published by Taylor & Francis in Journal of Liposome Research on 19 Oct 2016, available online: <a href="http://www.tandfonline.com/10.1080/08982104.2016.1239636">http://www.tandfonline.com/10.1080/08982104.2016.1239636</a>
Download date	2024-04-28 12:50:56
Item downloaded from	<a href="https://hdl.handle.net/10468/11059">https://hdl.handle.net/10468/11059</a>



## Enhanced skin deposition and delivery of voriconazole using ethosomal preparations

Waleed Faisal, Ghareb M. Soliman & Ahmed M. Hamdan

**To cite this article:** Waleed Faisal, Ghareb M. Soliman & Ahmed M. Hamdan (2016): Enhanced skin deposition and delivery of voriconazole using ethosomal preparations, Journal of Liposome Research, DOI: [10.1080/08982104.2016.1239636](https://doi.org/10.1080/08982104.2016.1239636)

**To link to this article:** <http://dx.doi.org/10.1080/08982104.2016.1239636>



Accepted author version posted online: 25 Sep 2016.



Submit your article to this journal [↗](#)



View related articles [↗](#)



View Crossmark data [↗](#)

## **Enhanced skin deposition and delivery of voriconazole using ethosomal preparations**

Waleed Faisal<sup>1</sup>, Ghareb M. Soliman<sup>2,3,\*</sup>, Ahmed M. Hamdan<sup>3</sup>

<sup>1</sup> *Department of Pharmaceutics, Faculty of Pharmacy, Minia University, Minia, Egypt*

<sup>2</sup> *Department of Pharmaceutics, Faculty of Pharmacy, Assiut University, Assiut, Egypt.*

<sup>3</sup> *Department of Pharmaceutics, Faculty of Pharmacy, University of Tabuk, Tabuk, Saudi Arabia*

Address for correspondence: Ghareb M. Soliman, Department of Pharmaceutics,  
Faculty of Pharmacy, Assiut University, Assiut, 71526, Egypt. Tel. +201013427311,  
E-mail: ghareb.soliman@aun.edu.eg

## Abstract

Despite its broad-spectrum antifungal properties, voriconazole has many side effects when administered systemically. The aim of this work was to develop an ethosomal topical delivery system for voriconazole and test its potential to enhance the antifungal properties and skin delivery of the drug. Voriconazole was encapsulated into various ethosomal preparations and the effect of phospholipid and ethanol concentrations on the ethosomes properties were evaluated. The ethosomes were evaluated for drug encapsulation efficiency, particle size and morphology and antifungal efficacy. Drug permeability and deposition were tested in rat abdominal skin. Drug encapsulation efficiency of up to 46% was obtained and it increased with increasing the phospholipid concentration whereas the opposite effect was observed for the ethanol concentration. The ethosomes had a size of 420-600 nm and negative zeta potential. The particle size of the ethosomes increased by increasing their ethanol content. The ethosomes achieved similar inhibition zones against *Aspergillus flavus* at a 2-fold lower drug concentration compared with drug solution in dimethyl sulfoxide. The *ex vivo* drug permeability through rat abdominal skin was ~6-fold higher for the ethosomes compared with the drug hydroalcoholic solution. Similarly, the amount of drug deposited in the skin was higher for the ethosomes and was dependent on the ethanol concentration of the ethosomes. These results confirm that voriconazole ethosomal preparations are promising topical delivery systems that can enhance the drug antifungal efficacy and improve its skin delivery.

**Keywords:** Voriconazole, ethosomes, skin permeability, topical delivery, *Aspergillus flavus*.

## Introduction

Voriconazole (VRC) is a broad-spectrum second-generation triazole antifungal agent derived from fluconazole (Maertens, 2004). This makes it active against all *Candida* species that are resistant to fluconazole (Nguyen and Yu, 1998). It is also effective against *Fusarium* species, endemic mycoses, including those that occur in the central nervous system, other hyaline molds, and many brown-black molds (Malani et al., 2015; Scott and Simpson, 2007). VRC was approved by the US food and drug administration in 2002 (Song et al., 2012). It is used as a first-line treatment for invasive aspergillosis, as well as other invasive fungal infections (Maschmeyer et al., 2007). Its mechanism of action involves the inhibition of cytochrome P450-dependent 14 $\alpha$ -lanosterol demethylation, which is a crucial step in cell membrane ergosterol synthesis (Johnson and Kauffman, 2003). VRC is fungistatic against *Candida* spp., whereas it is fungicidal against filamentous organisms such as *Aspergillus* species (Johnson and Kauffman, 2003; Scott and Simpson, 2007). VRC is also successfully used in the management of superficial fungal infections, such as fungal keratitis caused by *Beauveria bassiana*, cutaneous aspergillosis, *Candida albicans* keratitis and skin and nail fungal infections (Al-Badriyeh et al., 2009; de Sa et al., 2015; Klein and Blackwood, 2006; Lacroix and de Chauvin, 2008; Ogawa et al., 2016).

Although VRC is available in both parenteral and well-absorbed oral formulations, topical drug delivery is a better choice for the treatment of cutaneous fungal infections to increase drug efficacy and avoid the several side effects associated with systemic delivery. Thus, systemic VRC causes several side effects, such as blurred vision, skin rashes, elevated hepatic enzyme levels, nausea and vomiting, in addition to interaction with other drugs (Scott and Simpson, 2007). Side

effects on the liver include cholestasis, hepatocytolysis, or their combination (Mihaila, 2015). Because VRC is only available as tablets, oral suspension and injection, there is an unmet need for a topical drug delivery system to reduce the drug side effects and increase its efficacy. Careful review of the literature revealed only few studies reporting on the development of topical delivery systems for VRC (de Sa et al., 2015; El-Hadidy et al., 2012; Song et al., 2012; Song et al., 2014). Thus, liposomal VRC formulations were tested as a potential treatment of ocular fungal infections (de Sa et al., 2015). This formulation was able to deliver about  $47.85 \pm 5.72 \mu\text{g}/\text{cm}^2$  of drug into porcine cornea after 30 min of permeation test. VRC was also incorporated into transethosomes and its skin delivery was compared to deformable liposomes, conventional liposomes and ethosomes (Song et al., 2012). Transethosomes were better than other vesicular carriers in enhancing the skin permeation and skin deposition of VRC in the dermis/epidermis region.

Ethosomes are soft, malleable vesicles composed mainly of phospholipids, ethanol and water (Akhtar, 2014; Bragagni et al., 2012; Zhai et al., 2015). Ethosomes were initially developed by Touitou *et al.* to overcome the limited penetration of liposomes into the skin (Touitou et al., 2000a). They have the potential to overcome some problems associated with topical drug delivery arising not only from the physicochemical properties of the drug but also from the biological barriers where they have demonstrated superior drug delivery properties over other vesicular and conventional dosage forms (Ainbinder and Touitou, 2005; Garg et al., 2015; Khan et al., 2015; Mbah et al., 2014; Pandey et al., 2015). Liposomes are usually restricted to the upper layers of the skin whereas ethosomes have better ability to penetrate deeper in the skin layers and transport the incorporated drugs more effectively due to their high ethanolic contents and small size (Mbah et al., 2014). Ethanol acts by causing

disturbance of the skin lipid bilayer organization and therefore it enhances the ethosomes ability to penetrate the stratum corneum (Akhtar, 2014). The size of ethosomes is smaller than that of liposomes prepared under the same conditions due to the high alcohol content (Touitou et al., 2000a).

The aim of the present study was to prepare and characterize different VRC ethosomal formulations to enhance its skin delivery and improve its antifungal activity. The effect of different formulation variables on the vesicle properties and drug antifungal efficacy were evaluated. *Ex vivo* skin permeation and deposition of VRC were tested using rat abdominal skin and were compared with those of the drug hydroalcoholic solution.

## **Materials and methods**

### **Materials**

Phosphatidylcholine (Phospholipon 90H<sup>®</sup>; PL 90H) was purchased from Lipoid GmbH, D-67065 Ludwigshafen, Germany. Voriconazole (VRC) was purchased from Cerilliant, Round Rock, TX, USA. Dialysis membranes (Spectra/por, MWCO: 3.5-5 kDa, unless otherwise indicated) were purchased from Fisher Scientific (Rancho Dominguez, CA). Sabouraud's dextrose agar and HPLC grade acetonitrile were obtained from Sigma Aldrich, St. Louis, MO, USA. Absolute ethanol was purchased from Adwic, EL-Naser Pharmaceutical Co., Cairo, Egypt. All other chemicals were of reagent grade and used as received.

### **Solubility determination**

The aqueous solubility of VRC was determined by adding an excess amount of drug to 10 mL phosphate buffer (10 mM, pH 7.4) using a standardized shake flask method at 37°C with shake time of 48 h. Aliquot was then filtered through a 0.2 µm

membrane filter and the filtrate was assayed by HPLC to determine the drug concentration (described below).

### **Preparation of ethosomes**

VRC ethosomes were prepared by the cold method as described previously with slight modifications (Dayan and Touitou, 2000). The composition of the prepared ethosomes is given in Table 1. Briefly, VRC (0.5% w/v) and phospholipids (3-5% w/v) were dissolved in the designated amount of absolute ethanol (35-45%, v/v) and stirred using a magnetic stirrer for 5 min until complete dissolution was obtained. Absolute alcohol was used to avoid incorporation of uncalculated amounts of water in the formulation. Deionized water (QS to 100%) was slowly added to the magnetically stirred ethanolic mixture and the preparation was stirred at 700 RPM for 5 min at room temperature. Blank ethosomes were prepared following the same procedures and used as a control. The ethosomes were kept at 4 °C for further analysis.

### **Evaluation of the ethosomal preparations**

#### *Determination of VRC encapsulation efficiency*

The unencapsulated drug was separated from the ethosomes by centrifugation at 20,000 rpm and 4 °C for 30 min on a refrigerated centrifuge (Hettich, Germany). The clear supernatant was collected and aliquots were diluted 10 times by acetonitrile and the drug concentration was determined spectrophotometrically at absorbance  $\lambda_{\text{max}}$  of 256 nm and using a previously constructed calibration curve. VRC encapsulation efficiency was calculated from the following equation:

$$\text{VRC encapsulation efficiency (weight\%)} = \frac{T-C}{T} \times 100 \quad (1)$$

where T is the total amount of VRC used in the preparation, and C is the amount of drug in the supernatant (Fathalla et al., 2015; Maestrelli et al., 2009).



### *Visualization by transmission electron microscopy*

The formation of vesicular structures, as well as the morphology of the formed vesicles were examined by transmission electron microscope (TEM). TEM samples were prepared by adding 10  $\mu$ L of the ethosomal solution (Formulation F3) onto a Formvar-coated 400 mesh grid stabilized with evaporated carbon film. The samples were positively stained by adding 10  $\mu$ L of aqueous uranyl acetate solution. The samples were allowed to dry overnight at room temperature. Photos were then captured using Philips CM200 electron microscope equipped with an AMT 2k x 2k CCD camera at an acceleration voltage of 80 kV.

### *Determination of vesicle size and zeta potential*

The vesicle size, polydispersity index and zeta potential of different ethosomal preparations were determined using dynamic and electrophoretic light scattering using a Malvern Nano-ZetaSizer (Nano-ZS, Malvern Instruments, Worcestershire, UK). The instrument was equipped with a He-Ne laser operating at 633 nm and an avalanche photodiode detector. Aliquots of the ethosomal preparations were diluted (1:100) by the corresponding ethanol-water mixture used in their preparation. Measurements were performed in triplicate at room temperature 24 h after preparation. A cumulant analysis was applied to obtain the hydrodynamic diameter and polydispersity index of the ethosomes.

### ***In vitro* antifungal activity**

#### *Fungal strains*

*Asperigillus flavus* Assiut University Mycological Center (AUMC) # 1276 was used for this study. Clotrimazole was used as an antifungal standard. The mycelial mat was homogenized and filtered in sterile distilled water. The colony forming units (CFU) were counted by hemocytometer and adjusted to  $10^4$  CFU/mL.

### *Media*

Sabouraud's dextrose agar medium (10 g/L peptone from meat, 40 g/L glucose, 15 g/L agar) was prepared as previously described (Moss and McQuown, 1969). After sterilizing the medium and solidifying it in the plates, cork borer was used in order to make holes accepting 50  $\mu$ L of the tested solution.

### *Treatment*

To test the effect of drug concentration on its antifungal activity, *A. flavus* was treated with different concentrations of VRC encapsulated in ethosomes F3 (5000, 2500, 1250, 625, 312.5, 156.25, 78.125, 38.8, 19.5, 9.8, 4.9, 2.5  $\mu$ g/mL) and the diameter of the inhibition zones was measured. Similar drug concentrations in DMSO or hydroalcoholic solution (ethanol-water, 35:65, v/v) were also tested and used as control. The tested sample concentrations (50  $\mu$ L) were added to the holes in the culture plates and the plates were kept at  $28^{\circ}\text{C} \pm 2$  for 14 days. The inhibition zones were then measured. Three replicates were used for each concentration. DMSO alone and blank ethosomal preparations were used as negative controls.

### ***Ex vivo* drug permeation and skin deposition studies**

*Ex vivo* drug skin permeation study was carried out with rat abdominal skin using Franz's diffusion cell by the same method as described by Jain *et al.* (Jain et al., 2007). Wistar male albino rats (6–8 weeks old), weighing 120–150 g were used for procuring their abdominal skin. After removing the hair, the abdominal skin was separated from the underlying connective tissue with scalpel. The excised skin was placed on aluminum foil and any adhering fat and/or subcutaneous tissue was carefully removed from the dermal side of the skin. The skin was checked carefully to ensure that the skin samples were free from any surface irregularity, such as fine holes or crevices in the portions that were used for transdermal permeation studies. A preliminary wash of the skin was done with normal saline, followed by careful drying

between two filter papers. Skin was used directly without storage. All animals were treated in accordance with the ethical guidelines approved by Assiut University.

VRC permeation studies through rat abdominal skin were carried out using a receptor medium composed of pH 7.4 isotonic phosphate buffer containing 0.11% (w/v) formaldehyde as a preservative for the skin (Elsayed et al., 2006). Skin membranes were mounted between the donor and receptor compartments of diffusion cell with the stratum corneum side facing up. Formulations to be tested (F3, F6 and F9, equivalent to VRC 0.5% w/v) (0.5 mL) were applied to skin surface, which had an available diffusion area of  $3.14\text{ cm}^2$  and covered with aluminum foil to avoid diffusion medium evaporation. Diffusion medium (10 mL) was maintained at  $37^\circ\text{C}$  so that the membrane just touches the receptor medium surface. According to solubility data and the amount of the drug in each preparation, the receptor medium volume maintains sink conditions. Hydroalcoholic solution of VRC (0.5% w/v drug in 35% v/v ethanol/water mixture) was used as control ( $n = 3$ ). The diffusion medium was magnetically stirred at 100 rpm. The receptor medium was kept at  $37 \pm 1^\circ\text{C}$  throughout experiments. Half-milliliter samples of the receptor medium were removed at appropriate intervals (1, 2, 3, 4, 6, 8, and 24 h) and immediately replaced with fresh medium. VRC content of the samples was determined by HPLC. The cumulative amount of VRC permeated through rat skin (expressed as weight % of total VRC in the applied dose) was calculated and plotted as a function of time. The flux,  $J$  ( $\mu\text{g}/\text{cm}^2/\text{h}$ ) of each tested sample was calculated.

At the end of the drug permeation studies, the skin was used to determine the amount of drug deposited in rat skin. For this purpose, the skin was washed with water and kept in methanol as a drug extraction solvent for 24 h. The methanolic extract was filtered through  $0.2\text{ }\mu\text{m}$  filter and used to determine drug concentration by

HPLC. The cumulative amount of drug permeated through skin and the amount deposited in skin were plotted as a function of time. All experiments were done in triplicate.

### **HPLC assay of VRC**

HPLC assay of VRC was done according to previously reported procedures with slight modification (Khetre et al., 2009). The instrument used was a Y-Lin Technologies 9112 series HPLC system equipped with a Synergi, 2.6  $\mu$ m C18 reversed phase column (250 x 4.6 cm). Mobile phase consisted of acetonitrile:water (80:20, v/v) and the flow rate was maintained at 1.0 mL/min. Injection volume was 20  $\mu$ L and VRC was detected at 256 nm with a retention time of 4.6 min. A calibration curve ( $R^2 \geq 0.999$ ) of VRC was prepared using standard solutions ranging in concentration from 0.2 to 10  $\mu$ g/mL prepared immediately prior to the assay.

### **Statistical analysis**

All experiments were run in triplicate and results were expressed as mean  $\pm$  SD. Statistical data analysis was carried out using the Graph-Pad Prism version 5 software (USA). The data was analyzed by one-way analysis of variance (ANOVA) with Newman-Keuls post-hoc test. Statistical significance was predefined as  $p < 0.05$ .

## **Results and discussion**

### **Determination of voriconazole aqueous solubility**

The solubility of VRC in phosphate buffer pH 7.4 was found to be 0.7 mg/mL. This is much lower than the drug solubility at pH 1.2, which is reported to be around 3.2 mg/mL. VRC is a weakly basic drug with a  $pK_a$  of 4.8, which explains its much higher aqueous solubility in acidic media (Buchanan et al., 2007).

## **Preparation and characterization of VRC ethosomal preparations**

VRC loaded ethosomes were prepared by the cold method using different concentrations of phospholipids, ethanol and water (Table 1) and their different drug delivery aspects were studied. Although VRC-loaded ethosomes were prepared previously by Song et al., the main focus of that study was transethosomes with ethosomes being used as a control. Thus, the effects of different formulation variables on the ethosome properties and drug delivery potential were not revealed (Song et al., 2012). We selected the ethanol concentration in the range of 35-45%, v/v because it was reported that lower ethanol concentration negatively affected encapsulation efficiency of hydrophobic drugs while higher concentration could solubilize the phospholipid bilayers leading to leaky ethosomes and reduced drug loading (Abdulbaqi et al., 2016; Touitou et al., 2000b).

### **Size and shape of the prepared ethosomes**

Particle size and shape are known to affect vesicle physical stability and cellular uptake (Maestrelli et al., 2009). The particle size of blank ethosomes was  $97.7 \pm 1.2$  nm and it was significantly increased upon drug loading ( $p < 0.05$ ). Similar results were observed previously for paclitaxel-loaded ethosomes and were attributed to drug incorporation into the lipid bilayer (Paolino et al., 2012). This could lead to expansion of the lipid bilayer to accommodate the incorporated drug. Among the drug loaded formulations, the smallest size ( $423.67 \pm 26.64$  nm) was detected for formula F2 having lowest ethanol content (35%) and moderate phospholipid content (4%). The particle size of all the other formulations was within the 420-600 nm range (Table 2). There was a general increase in the particle size with the increase in the ethanol concentration in the ethosomes. For instance, the ethosome size increased from  $474.34 \pm 9.1$  (F1) to  $557.0 \pm 4.24$  nm (F4) upon increasing the ethanol concentration

from 35 to 40% at a constant phospholipid concentration of 3% (Table 2). In contrast, increasing the phospholipid concentration while keeping the ethanol concentration constant had a limited influence on the ethosome particle size (Table 2). These results are in agreement with previous reports (Touitou et al., 2000b). The polydispersity index of the prepared ethosomes was  $\sim 0.3$  for most of the formulations indicating fairly homogenous particle size distribution (Maestrelli et al., 2009; Mbah et al., 2014). The morphology of the vesicles was studied by TEM (formulation F3), which confirmed the formation of unilamellar vesicles having homogeneous and regular round shape (Figure 1). The size seen in the TEM picture (about 140 nm) is smaller than that obtained by DLS measurements (Table 2), probably due to ethosome drying during preparation for TEM measurements (Gao et al., 2013). It is noteworthy that DLS measures size of hydrated vesicles in aqueous solution while TEM measures that in the dry state.

Zeta potential of ethosomes is an important criterion that affects their stability and interaction with biological membranes (Touitou et al., 2000b). All the prepared ethosomes had a negative zeta potential ranging from  $\sim -10$  to  $-36$  mV (Table 2). This negative charge is attributed to the presence of ethanol in the ethosomes (Verma and Pathak, 2012). The magnitude of the ethosomes zeta potential was not affected by their composition. Interestingly, ethosomal preparations F3 kept at 4 °C for over six months did not show any signs of aggregation or fusion, a consequence of their negative surface charge (Bhosale and Avachat, 2013).

### **VRC encapsulation efficiency**

In order to reach the maximum drug encapsulation efficiency, the ethosomes were prepared at different phospholipid and ethanol concentrations. Table 2 shows that the drug encapsulation efficiency was dependent on the phospholipid

concentration, as well as the amount of ethanol used in the preparation. Thus, increasing the phospholipid concentration from 3 to 5% while keeping the ethanol content constant at 35% resulted in increasing the drug encapsulation efficiency from  $31.4 \pm 1.4$  to  $46.4 \pm 1.3\%$ . This positive effect of the phospholipid concentration on the drug encapsulation efficiency might be attributed to the hydrophobicity of the drug, which facilitate hydrophobic interactions with the vesicle membranes and thus, enhance drug encapsulation efficiency. Similar trend was previously reported in other studies (Bhosale and Avachat, 2013; Fathalla et al., 2015; Maheshwari et al., 2012). Contrary to the phospholipid concentration effect, increasing the ethanol concentration in the ethosomes resulted in decreasing the drug encapsulation efficiency (Table 2). Thus, increasing the ethanol content from 35 to 45% while keeping the phospholipid content constant at 3% resulted in decreasing VRC encapsulation efficiency from  $31.4 \pm 1.4$  to  $22.2 \pm 1.1\%$ . This might be attributed to the increased fluidity and permeability of the vesicular membrane and increased solubility of the drug in ethanol leading to drug loss from the vesicles during preparation (Bhosale and Avachat, 2013; Maheshwari et al., 2012; Verma and Pathak, 2012).

### ***In vitro* antifungal activity**

In order to confirm the potential of VRC ethosomes to enhance the drug antifungal activity and reduce the required concentration, the drug-loaded ethosomes (F3) were serially diluted and the minimum concentration that gave measurable inhibition zones against *Asperigillus flavus* was recorded. The formulation F3 was selected on the basis of high drug encapsulation efficiency (~ 46%, Table 2). The results were compared with similarly treated VRC solution in DMSO (0.5%, w/v) and VRC solution in ethanol-water mixture (35:65, v/v) (0.5% w/v). Blank ethosomes and DMSO alone were used as a control. DMSO drug solution has no clinical relevance

but it was used here for comparison only since the limited aqueous solubility of the drug prevented preparation of aqueous solution. Care was taken to ensure that all the tested formulations have the same drug concentration (0.5% w/v). No inhibition zones were observed for blank ethosomes. The inhibition zone of DMSO alone was less than 4 mm. VRC solution in DMSO continued to be active against *A. flavus* up to 5 dilutions (156.25 µg/mL) which gave an inhibition zone ~20 mm, after which no inhibition zone was detectable (Table 3). Interestingly, the ethosomal drug preparation (F3) had a similar inhibition zone against *A. flavus* (~20 mm) at a 2-fold lower drug concentration (Table 3). Thus, similar inhibition zones were detected for VRC DMSO solution (VRC concentration of 156.25 µg/mL) and ethosomal VRC (F3) (VRC concentration of 78.13 µg/mL) (Table 3, Figure 2). This is a very promising finding since drug antifungal activity can be achieved at much lower drug concentration. Lower drug concentrations decrease the incidence and severity of side effects, reduce economic burden of the treatment, improve patient compliance and leads to better therapeutic outcome (Mbah et al., 2014). However, the VRC hydroalcoholic solution was more active than the VRC ethosomes where similar inhibition zone was observed for a VRC concentration that is two times less than that in ethosomes. This might be attributed to better diffusion of the drug in hydroalcoholic solution since the drug in ethosomes will need to be released from the ethosome first to be active.

#### ***Ex vivo* drug permeability study**

The investigation of transport enhancement ability of ethosomal formulations (F3, F6, and F9) was measured using rat abdominal skin. These formulations were selected on the basis of high drug encapsulation efficiency (F3) (~ 46%, Table 2) and to test the effect of ethanol concentration of the drug permeability (ethanol concentration increased from 35 to 45% from F3 to F9, Table 1). Figure 3 shows the



cumulative amount of VRC permeated across excised rat skin as a function of time. The cumulative amount of drug that permeated the skin after 24 h was significantly higher for all the tested ethosomes compared to the drug hydroalcoholic solution ( $p<0.05$ ). Among the tested ethosomal formulations, F3 showed significantly higher drug permeation ( $23.5\pm2.4\%$ ) compared to F6 ( $17.6\pm1.8\%$ ) and F9 ( $16\pm1.6\%$ ) ( $p<0.05$ ). The difference between the drug permeability from F6 and F9 was not significant ( $p>0.05$ ). Although the effect of ethanol as a permeation enhancer is well known, the higher drug permeation from the ethosomal formulations compared to the drug hydroalcoholic solution suggests some kind of synergistic enhancement mechanism between ethanol, ethosomes components and skin phospholipids (Berner and Liu, 1955; Touitou et al., 2000a). Ethanol has a softening effect on the phospholipids in ethosomes, which might make the vesicles more flexible and soft thus, allowing better penetration into deeper layers of the skin (Touitou et al., 2000a). Interaction of ethanol and ethosome phospholipids with the stratum corneum lipids and the subsequent modification of the intercellular lipid lamellae might also contribute to the enhanced permeability observed for drug-loaded ethosomes (Blume et al., 1993; Campani et al., 2016; Touitou et al., 2000a). This facilitates penetration of the drug molecules into and across the stratum corneum (Honeywell-Nguyen and Bouwstra, 2003; Honeywell-Nguyen et al., 2002). Similar enhancement in the drug permeation across the skin was previously reported for the drug-loaded ethosomes compared to drug hydroalcoholic solutions (Campani et al., 2016; Dayan and Touitou, 2000; Touitou et al., 2000a).

Further, drug flux from different ethosomes across rat abdominal skin was calculated and compared with that for drug hydroalcoholic solution. The transdermal flux of the drug from ethosomes F3 ( $22\pm2.1 \mu\text{g}/\text{cm}^2/\text{h}$ ) was observed to be

significantly higher than from ethosomes F6 ( $16.6 \pm 1.5 \mu\text{g}/\text{cm}^2/\text{h}$ ) and ethosomes F9 ( $15.2 \pm 1.6 \mu\text{g}/\text{cm}^2/\text{h}$ ) ( $p < 0.05$ ). Transdermal drug flux from VRC hydroalcoholic solution was  $3.7 \pm 0.4 \mu\text{g}/\text{cm}^2/\text{h}$ . This confirms that the drug transdermal flux from ethosomes was  $\sim 4.1$ - $5.9$ -fold higher than that from hydroalcoholic solution. When comparing the flux from different ethosomal formulations, it is noticed that the flux rate increases when the concentration gradient builds up at the application site, i.e. the highest flux rate was obtained for the formulation having the highest drug encapsulation efficiency (i.e., F3, % encapsulation efficiency  $46.4 \pm 1.2$ , Table 2). Stratum corneum provides the rate-limiting step in percutaneous absorption and the inclusion of a penetration enhancer such as ethanol might play a role in the enhanced skin delivery of lipophilic drugs; yet, it is not the sole factor operating (El Maghraby, 2008; El Maghraby et al., 2015). The drug encapsulated into vesicular lipid bilayers might bypass the primary barrier for drug permeation, and this effect is expected to have a more important role in improving both skin deposition and transdermal permeation than the ethanol effect (Elsayed et al., 2006). This assumption is supported by the observation that the ethosomal formulations had a much higher VRC flux than the drug hydroalcoholic solution. Moreover, our results showed that the flux decreased with increasing ethanol concentration ( $F3 > F6 > F9$ ). This might be attributed to the deteriorating effect of ethanol on the lipid bilayers at higher concentrations (Jain et al., 2007).

Skin deposition of the drug from different formulations was also investigated (Figure 4). The amount of the drug deposited in skin after 24 h was significantly higher for ethosomes F3 ( $42.9 \pm 4.1\%$ ) when compared with F6 ( $32.3 \pm 2.8\%$ ) and F9 ( $29.7 \pm 3.4\%$ ) ( $p < 0.05$ ). Further, the amount of drug deposited in skin from the hydroalcoholic solution ( $7.2 \pm 0.8\%$ ) was significantly lower than that from any of the

tested ethosomal formulations ( $p<0.05$ ). This enhanced skin deposition for the drug loaded into the ethosomes might be attributed to the penetration and deposition of the vesicles into the skin layers with the vesicles acting as a reservoir for continuous drug delivery (Ascenso et al., 2015; Campani et al., 2016).

It was suggested that the high percentage of alcohol in donor compartment may diffuse through skin and extract deposited drug, and thus lead to decreased skin deposition and skin penetration with increasing the alcohol content of the ethosomes (F3 to F9, Table 1). Deteriorating effect of ethanol on the lipid bilayers at a higher concentration could also limit the absorption efficacy. Likewise, the entrapment efficiency of ethosomes F6 and F9 were similar, however, the slightly higher drug deposition into rat abdominal skin observed with F6 may also be attributed to the lower percentage of ethanol (Figure 4, Table 1).

## Conclusion

Voriconazole was efficiently loaded into ethosomal preparation with an encapsulation efficiency of up to ~ 46%. The encapsulation efficiency increased with increasing the phospholipid concentration but decreased with increasing the alcohol concentration. The formed ethosomes had a spherical shape and were uniform in size and shape. The particle size was in the nanometer range and they had a negative surface charge. The antifungal properties of the optimal ethosomal formulation were tested against *A. flavus* and compared with the drug DMSO solution and hydroalcoholic solution. The drug ethosomal solution was more active than the drug in DMSO but less active than the drug hydroalcoholic solution. *Ex vivo* permeability studies showed that ethosomal formulation F3 had ~6-fold enhancement in the amount of drug permeated across rat abdominal skin compared to the drug hydroalcoholic solution. The amount of drug deposited in the skin was also higher for

the ethosomal formulations compared to the hydroalcoholic solution, and was higher for the ethosomal formulations having lower ethanol content. These results confirm the potential of ethosomal preparations as efficient delivery system for voriconazole for the treatment of topical fungal infections.

### **Conflict of interest**

The authors report no conflicts of interest.

### **References**

- Abdulbaqi IM, Darwis Y, Khan NA, Assi RA, Khan AA. (2016). Ethosomal nanocarriers: the impact of constituents and formulation techniques on ethosomal properties, in vivo studies, and clinical trials. *Int J Nanomed* 11: 2279-2304.
- Ainbinder D, Touitou E. (2005). Testosterone ethosomes for enhanced transdermal delivery. *Drug Deliv* 12: 297-303.
- Akhtar N. (2014). Vesicles: a recently developed novel carrier for enhanced topical drug delivery. *Curr Drug Deliv* 11: 87-97.
- Al-Badriyeh D, Leung L, Davies GE, Stewart K, Kong D. (2009). Successful use of topical voriconazole 1% alone as first-line antifungal therapy against *Candida albicans* keratitis. *Ann Pharmacother* 43: 2103-2107.
- Ascenso A, Raposo S, Batista C, Cardoso P, Mendes T, Praca FG, Bentley MV, Simoes S. (2015). Development, characterization, and skin delivery studies of related ultradeformable vesicles: transfersomes, ethosomes, and transethosomes. *Int J Nanomed* 10: 5837-5851.
- Berner B, Liu P. (1955). Alcohols, in: E.W. Smith, E.W., Maibach, H.I. (Eds.), *Percutaneous Penetration Enhancers*. CRC Press, Boca Raton, pp. 45-60.
- Bhosale SS, Avachat AM. (2013). Design and development of ethosomal transdermal drug delivery system of valsartan with preclinical assessment in Wistar albino rats. *J Liposome Res* 23: 119-125.
- Blume A, Jansen M, Ghyczy M, Gareiss J. (1993). Interaction of phospholipid liposomes with lipid model mixtures for stratum corneum lipids. *Int J Pharm* 99: 219-228.
- Bragagni M, Mennini N, Maestrelli F, Cirri M, Mura P. (2012). Comparative study of liposomes, transfersomes and ethosomes as carriers for improving topical delivery of celecoxib. *Drug Deliv* 19: 354-361.
- Buchanan C, Buchanan N, Edgar K, Ramsey M. (2007). Solubility and dissolution studies of antifungal drug: hydroxybutenyl- $\beta$ -cyclodextrin complexes. *Cellulose* 14: 35-47.
- Campani V, Biondi M, Mayol L, Cilurzo F, Franze S, Pitaro M, De Rosa G. (2016). Nanocarriers to enhance the accumulation of vitamin K1 into the skin. *Pharm Res* 33: 893-908.
- Dayan N, Touitou E. (2000). Carriers for skin delivery of trihexyphenidyl HCl: ethosomes vs. liposomes. *Biomaterials* 21: 1879-1885.
- de Sa FA, Taveira SF, Gelfuso GM, Lima EM, Gratieri T. (2015). Liposomal voriconazole (VOR) formulation for improved ocular delivery. *Colloids Surf B Biointerfaces* 133: 331-338.

- El-Hadidy GN, Ibrahim HK, Mohamed MI, El-Milligi MF. (2012). Microemulsions as vehicles for topical administration of voriconazole: formulation and in vitro evaluation. *Drug Dev Ind Pharm* 38: 64-72.
- El Maghraby GM. (2008). Transdermal delivery of hydrocortisone from eucalyptus oil microemulsion: effects of cosurfactants. *Int J Pharm* 355: 285-292.
- El Maghraby GM, Ahmed AA, Osman MA. (2015). Penetration enhancers in proniosomes as a new strategy for enhanced transdermal drug delivery. *Saudi Pharm J* 23: 67-74.
- Elsayed MM, Abdallah OY, Naggar VF, Khalafallah NM. (2006). Deformable liposomes and ethosomes: mechanism of enhanced skin delivery. *Int J Pharm* 322: 60-66.
- Fathalla D, Soliman G, Fouad E. (2015). Development and in vitro/in vivo evaluation of liposomal gels for the sustained ocular delivery of latanoprost. *J Clin Exp Ophthalmol* 6: 2.
- Gao X, Wang B, Wei X, Rao W, Ai F, Zhao F, Men K, Yang B, Liu X, Huang M, Gou M, Qian Z, Huang N, Wei Y. (2013). Preparation, characterization and application of star-shaped PCL/PEG micelles for the delivery of doxorubicin in the treatment of colon cancer. *Int J Nanomed* 8: 971-982.
- Garg BJ, Garg NK, Beg S, Singh B, Katare OP. (2015). Nanosized ethosomes-based hydrogel formulations of methoxsalen for enhanced topical delivery against vitiligo: formulation optimization, in vitro evaluation and preclinical assessment. *J Drug Target* 12: 1-14.
- Honeywell-Nguyen PL, Bouwstra JA. (2003). The in vitro transport of pergolide from surfactant-based elastic vesicles through human skin: a suggested mechanism of action. *J Control Release* 86: 145-156.
- Honeywell-Nguyen PL, Frederik PM, Bomans PH, Junginger HE, Bouwstra JA. (2002). Transdermal delivery of pergolide from surfactant-based elastic and rigid vesicles: characterization and in vitro transport studies. *Pharm Res* 19: 991-997.
- Jain S, Tiwary AK, Sapra B, Jain NK. (2007). Formulation and evaluation of ethosomes for transdermal delivery of lamivudine. *AAPS PharmSciTech* 8: E111.
- Johnson LB, Kauffman CA. (2003). Voriconazole: a new triazole antifungal agent. *Clin Infect Dis* 36: 630-637.
- Khan NR, Harun MS, Nawaz A, Harjoh N, Wong TW. (2015). Nanocarriers and their Actions to Improve Skin Permeability and Transdermal Drug Delivery. *Curr Pharm Des* 21: 2848-2866.
- Khetre AB, Sinha PK, Damle MC, Mehendre R. (2009). Development and validation of stability indicating RP-HPLC method for voriconazole. *Indian journal of pharmaceutical sciences* 71: 509-514.
- Klein KC, Blackwood RA. (2006). Topical voriconazole solution for cutaneous aspergillosis in a pediatric patient after bone marrow transplant. *Pediatrics* 118: e506-508.
- Lacroix C, de Chauvin MF. (2008). In vitro activity of amphotericin B, itraconazole, voriconazole, posaconazole, caspofungin and terbinafine against *Scytalidium dimidiatum* and *Scytalidium hyalinum* clinical isolates. *J Antimicrob Chemother* 61: 835-837.
- Maertens JA. (2004). History of the development of azole derivatives. *Clin Microbiol Infect* 10 Suppl 1: 1-10.

- Maestrelli F, Capasso G, Gonzalez-Rodriguez ML, Rabasco AM, Ghelardini C, Mura P. (2009). Effect of preparation technique on the properties and in vivo efficacy of benzocaine-loaded ethosomes. *J Liposome Res* 19: 253-260.
- Maheshwari RG, Tekade RK, Sharma PA, Darwhekar G, Tyagi A, Patel RP, Jain DK. (2012). Ethosomes and ultradeformable liposomes for transdermal delivery of clotrimazole: A comparative assessment. *Saudi Pharm J* 20: 161-170.
- Malani AN, Kerr LE, Kauffman CA. (2015). Voriconazole: How to use this antifungal agent and what to expect. *Semin Respir Crit Care Med* 36: 786-795.
- Maschmeyer G, Haas A, Cornely OA. (2007). Invasive aspergillosis: epidemiology, diagnosis and management in immunocompromised patients. *Drugs* 67: 1567-1601.
- Mbah CC, Builders PF, Attama AA. (2014). Nanovesicular carriers as alternative drug delivery systems: ethosomes in focus. *Expert Opin Drug Deliv* 11: 45-59.
- Mihaila RG. (2015). Voriconazole and the liver. *World J Hepatol* 7: 1828-1833.
- Moss ES, McQuown AL. (1969). *Atlas of Medical Mycology*, 3rd edition ed. Williams & Wilkins Co., Baltimore.
- Nguyen MH, Yu CY. (1998). Voriconazole against fluconazole-susceptible and resistant candida isolates: in-vitro efficacy compared with that of itraconazole and ketoconazole. *J Antimicrob Chemother* 42: 253-256.
- Ogawa A, Matsumoto Y, Yaguchi T, Shimmura S, Tsubota K. (2016). Successful treatment of *Beauveria bassiana* fungal keratitis with topical voriconazole. *J Infect Chemother* 22: 257-260.
- Pandey V, Golhani D, Shukla R. (2015). Ethosomes: versatile vesicular carriers for efficient transdermal delivery of therapeutic agents. *Drug Deliv* 22: 988-1002.
- Paolino D, Celia C, Trapasso E, Cilurzo F, Fresta M. (2012). Paclitaxel-loaded ethosomes(R): potential treatment of squamous cell carcinoma, a malignant transformation of actinic keratoses. *Eur J Pharm Biopharm* 81: 102-112.
- Scott LJ, Simpson D. (2007). Voriconazole : a review of its use in the management of invasive fungal infections. *Drugs* 67: 269-298.
- Song CK, Balakrishnan P, Shim CK, Chung SJ, Chong S, Kim DD. (2012). A novel vesicular carrier, transethosome, for enhanced skin delivery of voriconazole: characterization and in vitro/in vivo evaluation. *Colloids Surf B Biointerfaces* 92: 299-304.
- Song SH, Lee KM, Kang JB, Lee SG, Kang MJ, Choi YW. (2014). Improved skin delivery of voriconazole with a nanostructured lipid carrier-based hydrogel formulation. *Chem Pharm Bull (Tokyo)* 62: 793-798.
- Touitou E, Dayan N, Bergelson L, Godin B, Eliaz M. (2000a). Ethosomes - novel vesicular carriers for enhanced delivery: characterization and skin penetration properties. *J Control Release* 65: 403-418.
- Touitou E, Dayan N, Bergelson L, Godin B, Eliaz M. (2000b). Ethosomes — novel vesicular carriers for enhanced delivery: characterization and skin penetration properties. *J Control Release* 65: 403-418.
- Verma P, Pathak K. (2012). Nanosized ethanolic vesicles loaded with econazole nitrate for the treatment of deep fungal infections through topical gel formulation. *Nanomedicine* 8: 489-496.
- Zhai Y, Xu R, Wang Y, Liu J, Wang Z, Zhai G. (2015). Ethosomes for skin delivery of ropivacaine: preparation, characterization and ex vivo penetration properties. *J Liposome Res* 25: 316-324.

Table 1. Composition of different voriconazole ethosomal formulations.

Formula	F1	F2	F3	F4	F5	F6	F7	F8	F9
VRC (% , w/v)	0.5	0.5	0.5	0.5	0.5	0.5	0.5	0.5	0.5
Phospholipid (% , w/v)	3	4	5	3	4	5	3	4	5
Ethanol (% , v/v)	35	35	35	40	40	40	45	45	45
Distilled water (%)	q.s. up to 100%								

Table 2. Drug encapsulation efficiency, vesicular size and polydispersity index of different ethosomal preparations.

Formula	Encapsulation efficiency (%) <sup>a</sup>	Vesicle size <sup>b</sup> (nm)	PDI <sup>c</sup>	Zeta potential (mV)
Blank vesicles	0	97.7±1.2	0.3±0.02	-8.5±0.35
F1	31.4±1.4	474.34±9.1	0.29±0.05	-9.40±0.20
F2	46.5±2.1	423.67±26.64	0.28±0.06	-18.20±0.30
F3	46.4±1.3	459.0±19.30	0.32±0.20	-16.76±0.11
F4	29.8±6.6	557.0±4.24	0.35±0.09	-36.65±0.92
F5	36.8±1.3	551.0±13.1	0.36±0.07	-10.76±0.11
F6	38.1±1.3	572.0±8.0	0.39±0.07	-17.23±0.20
F7	22.2±1.1	561.0±14.1	0.38±0.01	-8.66±0.11
F8	29.3±1.6	526.34±14.84	0.56±0.01	-21.43±0.30
F9	38.7±1.3	599.67±14.46	0.42±0.06	-19.43±0.46

<sup>a</sup> Percent drug encapsulation efficiency, calculated from equation (1), mean of three different measurements ±SD.

<sup>b</sup> Vesicle size (nm), mean of three different measurements ±SD.

<sup>c</sup> PDI, polydispersity index, mean of three different measurements ±SD.

Table 3. Inhibition zone (mm) of different concentrations of voriconazole ethosomes (F3) and voriconazole solution in DMSO against *A. flavus*

Concentration ( $\mu\text{g/mL}$ )	Inhibition zone (mm)		
	VRC in DMSO	VRC hydroalcoholic solution	Ethosomes (F3)
5000	52.67 $\pm$ 0.58	50.67 $\pm$ 1.15	50.67 $\pm$ 1.15
2500	50.00 $\pm$ 0.00	50.67 $\pm$ 1.15	50.00 $\pm$ 0.00
1250	46.00 $\pm$ 1.0	46.67 $\pm$ 1.15	49.33 $\pm$ 1.15
625	40.33 $\pm$ 0.58	44.00 $\pm$ 0.00	43.33 $\pm$ 1.15
312.50	30.67 $\pm$ 1.15	36.33 $\pm$ 1.53	39.33 $\pm$ 1.15
156.25	20.00 $\pm$ 0.00	31.33 $\pm$ 1.53	34.67 $\pm$ 1.15
78.13	0	22.67 $\pm$ 1.15	21.00 $\pm$ 1.00
39.06	0	10.67 $\pm$ 1.15	0



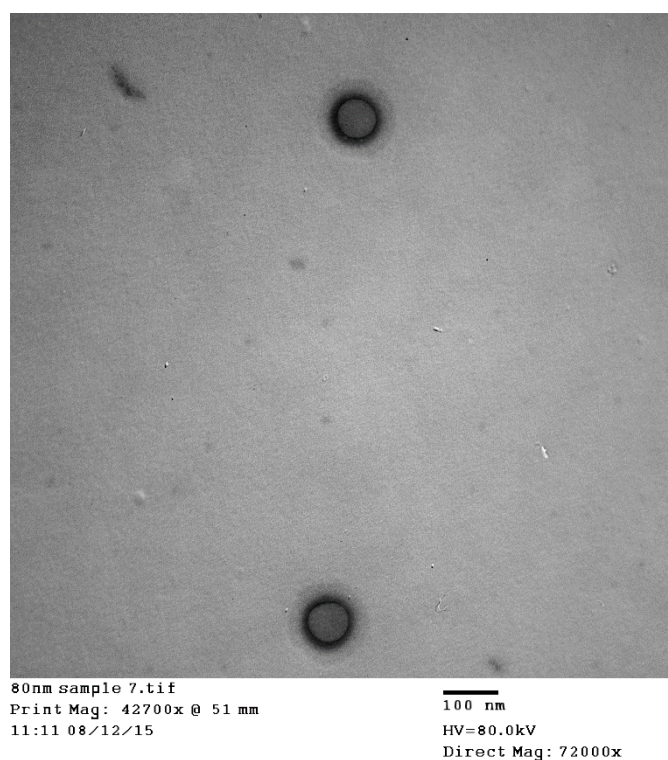


Figure 1. TEM image of voriconazole-loaded ethosomes (formulation F3).

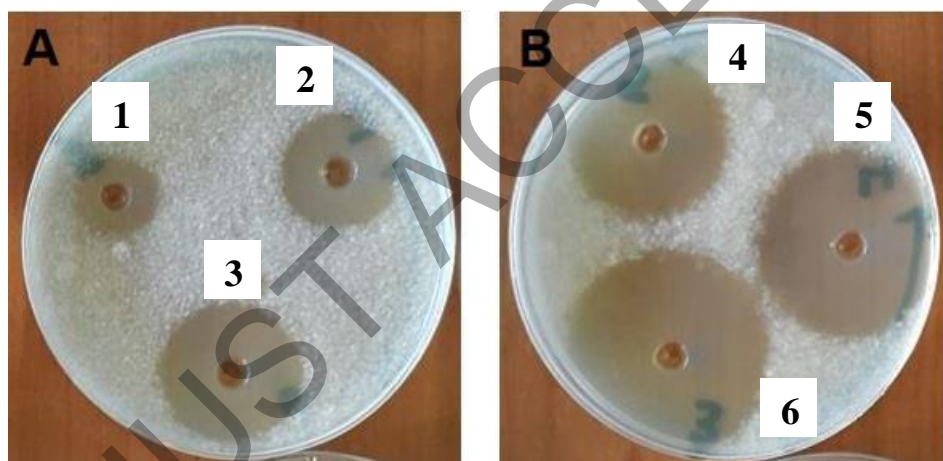


Figure 2. Inhibition zones of different concentrations of VRC ethosomal solution (F3) against *Asperigillus flavus*. (1) 78  $\mu\text{g/mL}$ , (2) 156.25  $\mu\text{g/mL}$ , (3) 312.5  $\mu\text{g/mL}$ , (4) 625  $\mu\text{g/mL}$ , (5) 1250  $\mu\text{g/mL}$  and (6) 2500  $\mu\text{g/mL}$ . Culture plates were kept at  $28^{\circ}\text{C} \pm 2$  for 14 days.

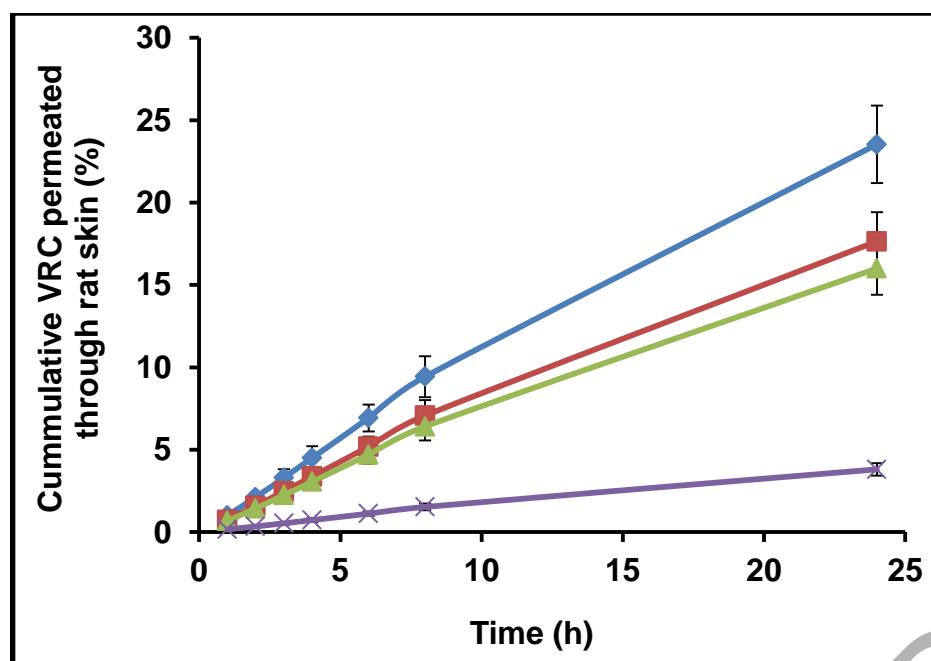


Figure 3. *Ex vivo* cumulative amount of VRC permeated through rat abdominal skin from ethosomes (F3 (♦), F6 (■), F9 (▲)) and from hydroalcoholic solution (x) over 24 h. Data are expressed as weight % of total VRC in the applied dose (mean±SD, n = 3).

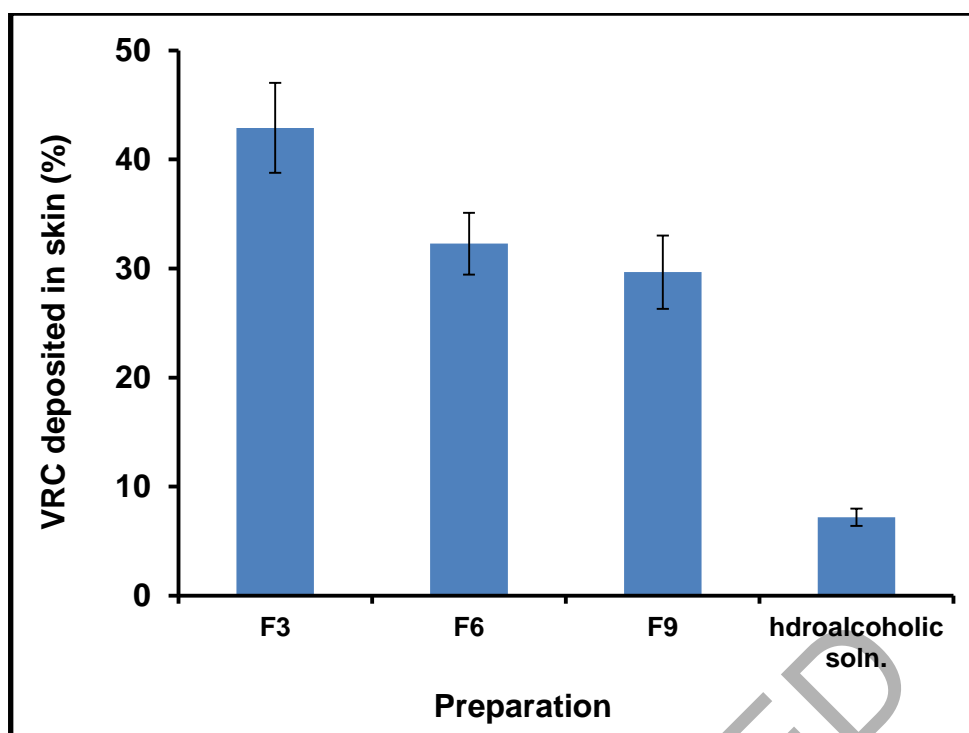


Figure 4. *Ex vivo* deposition of VRC in rat abdominal skin after 24 h of application of ethosomes (F3, F6 and F9) and drug hydroalcoholic solution. Data are expressed as % of total VRC in the applied dose (mean $\pm$ SD, n = 3).